SCIENTIFIC REPORTS

OPEN

SUBJECT AREAS:
ENVIRONMENTAL SCIENCES
CHEMISTRY

Received
30 April 2014

Accepted
3 October 2014

Published
22 October 2014

First retrieval of hourly atmospheric radionuclides just after the Fukushima accident by analyzing filter-tapes of operational air pollution monitoring stations

Haruo Tsuruta[1], Yasuji Oura[2], Mitsuru Ebihara[2], Toshimasa Ohara[3] & Teruyuki Nakajima[1]

[1]Atmosphere and Ocean Research Institute, The University of Tokyo, Kashiwa, Japan, [2]Department of Chemistry, Tokyo Metropolitan University, Tokyo, Japan, [3]Fukushima Project Office, National Institute for Environmental Studies, Tsukuba, Japan.

Correspondence and requests for materials should be addressed to H.T. (haru2004@aori.u-tokyo.ac.jp)

No observed data have been found in the Fukushima Prefecture (FP) for the time-series of atmospheric radionuclides concentrations just after the Fukushima Daiichi Nuclear Power Plant (FD1NPP) accident. Accordingly, current estimates of internal radiation doses from inhalation, and atmospheric radionuclide concentrations by atmospheric transport models are highly uncertain. Here, we present a new method for retrieving the hourly atmospheric ^{137}Cs concentrations by measuring the radioactivity of suspended particulate matter (SPM) collected on filter tapes in SPM monitors which were operated even after the accident. This new dataset focused on the period of March 12–23, 2011 just after the accident, when massive radioactive materials were released from the FD1NPP to the atmosphere. Overall, 40 sites of the more than 400 sites in the air quality monitoring stations in eastern Japan were studied. For the first time, we show the spatio-temporal variation of atmospheric ^{137}Cs concentrations in the FP and the Tokyo Metropolitan Area (TMA) located more than 170 km southwest of the FD1NPP. The comprehensive dataset revealed how the polluted air masses were transported to the FP and TMA, and can be used to re-evaluate internal exposure, time-series radionuclides release rates, and atmospheric transport models.

Many measurements were made for radiation dose rates at monitoring posts and the deposition densities of radionuclides on the ground in eastern Japan just after the Fukushima Daiichi Nuclear Power Plant (FD1NPP) accident on March 11, 2011[1–5]. In contrast, a time series of atmospheric radionuclide concentrations in an early period after the accident has not been found in the Fukushima Prefecture (FP), and little data were found in the Tokyo Metropolitan Area (TMA)[6,7]. Consequently, the estimated time-series release rates of radionuclides from the FD1NPP just after the accident are largely uncertain[8–14], because only radiation dose rates and/or the very limited data of atmospheric radionuclides have been available. In addition, atmospheric radionuclide concentrations simulated at a regional/global scale by atmospheric transport models with a source term, have also large uncertainty, due to a lack of observed data for validation[15–24]. Furthermore, the estimates of internal radiation dose rates from inhalation for health risk assessments have resulted in much uncertainty[25–30], because initial atmospheric radionuclide concentrations have not been found for inhalation. Although the observed deposition densities of radionuclides on the ground were used to estimate internal radiation doses in some cases[25,28], the time integrated atmospheric radionuclide concentrations for inhalation[31] derived from these estimates would be substantially underestimated if the polluted air masses passed without precipitation.

In the meantime, suspended particulate matter (SPM) mass concentrations are routinely measured at air quality monitoring sites in Japan, which are mainly located in urban/industrial areas as directed by the national air pollution control act (Fig. 1a). We obtained used filter tapes on which SPM was collected every hour by SPM mass monitors, from more than 400 sites in eastern Japan. Then, to retrieve the hourly transport of the polluted air masses with high radioactive material concentrations, the radionuclides were measured for about 6300 samples of hourly SPM at 16 and 24 sites in the FP and TMA, respectively, between March 12 and March 23, 2011 just after the accident (Fig. 1b and c). As a result, 37 data sets of ^{137}Cs concentrations from 40 SPM sites were studied (Table

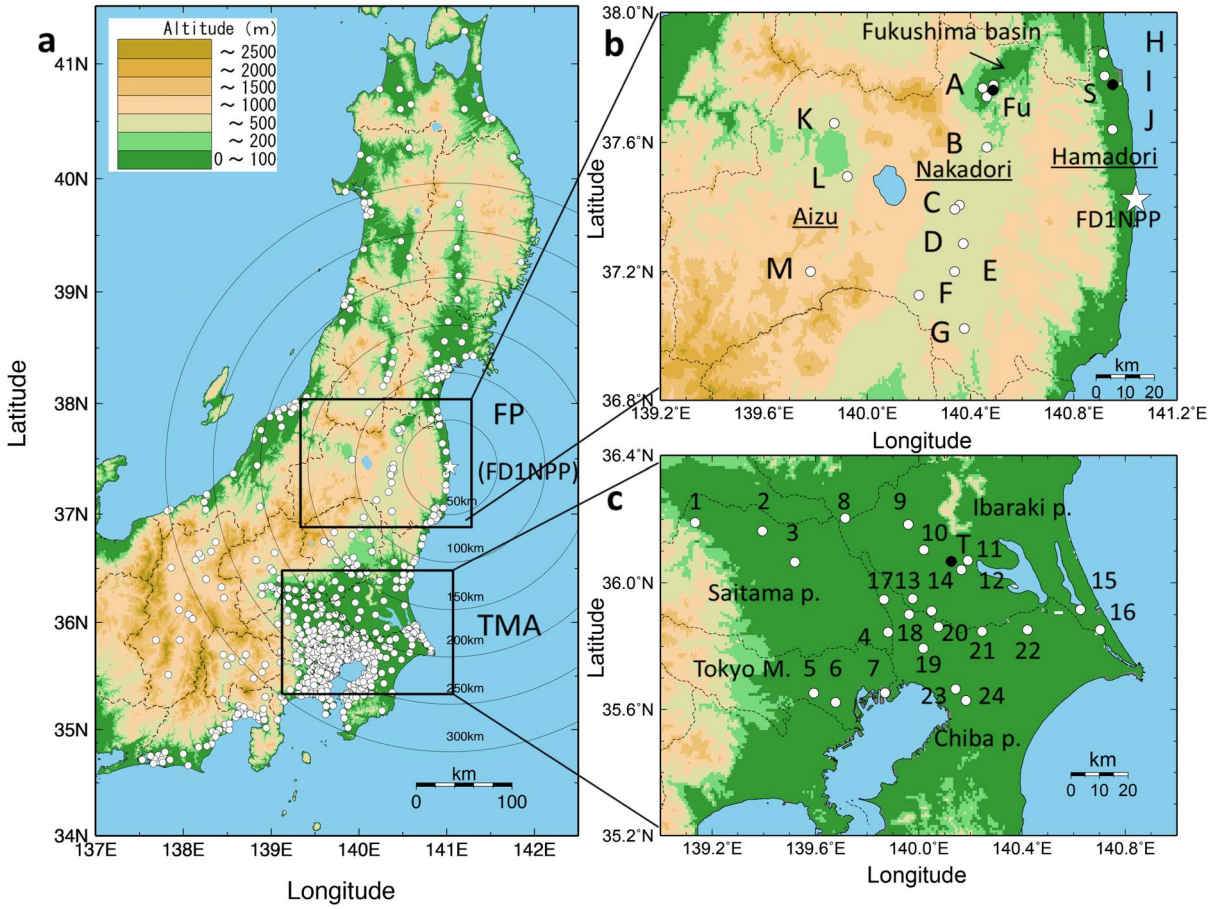

Figure 1 | Map of the SPM monitoring sites. (a), SPM monitoring sites (open circle) managed and maintained by local governments in eastern Japan before the accident. (b), Map of 16 SPM sites (open circle) in the FP for the ^{137}Cs measurement in this study. The site of A and C has 3 and 2 SPM monitoring sites, respectively. (c), Map of 24 sites (open circle) in the TMA for the ^{137}Cs measurement in this study. The Fu, S, and T site (black dot) corresponds to the Fukushima, Soma, and Tsukuba meteorological station, respectively. The mapping of a to c was made by using the Generic Mapping Tools (GMT)[39] and the topography data of Global 30 Arc-Second Elevation (GTOPO30)[40].

S1). In this paper, only the atmospheric ^{137}Cs concentrations are shown, because the activity of ^{134}Cs was nearly equal to that of ^{137}Cs in the FD1NPP accident, and ^{131}I was not detected after more than one year due to its short half-life of 8 days.

Results

The atmospheric ^{137}Cs concentrations more than 10 Bq m^{-3} were frequently measured at the SPM sites in the period of March 12–23 except two days when westerly winds were prevailing to transport the

Table 1 | Days and areas of the transport of polluted air masses (P1 to P9) with high ^{137}Cs

	Day of March, 2011										Area		
No.	12	13	14	15	16	17	18	19	20	21	N. Hamadori	Nakadori	TMA
P1	●	→									●		
P2				●									●
P3				●	→						○	●	
P4					●								●
P5							●				●		
P6								●			●		
P7									○				○
P8									●	→	●	○	
P9										●			●

No., Number of major plume transport from the FD1NPP just after the accident; N., Northern; TMA, Tokyo Metropolitan Area; ●, The maximum ^{137}Cs concentration>100 Bq m^{-3}; ○, The maximum ^{137}Cs concentration<100 Bq m^{-3}; →, High ^{137}Cs concentrations continued to the following morning.

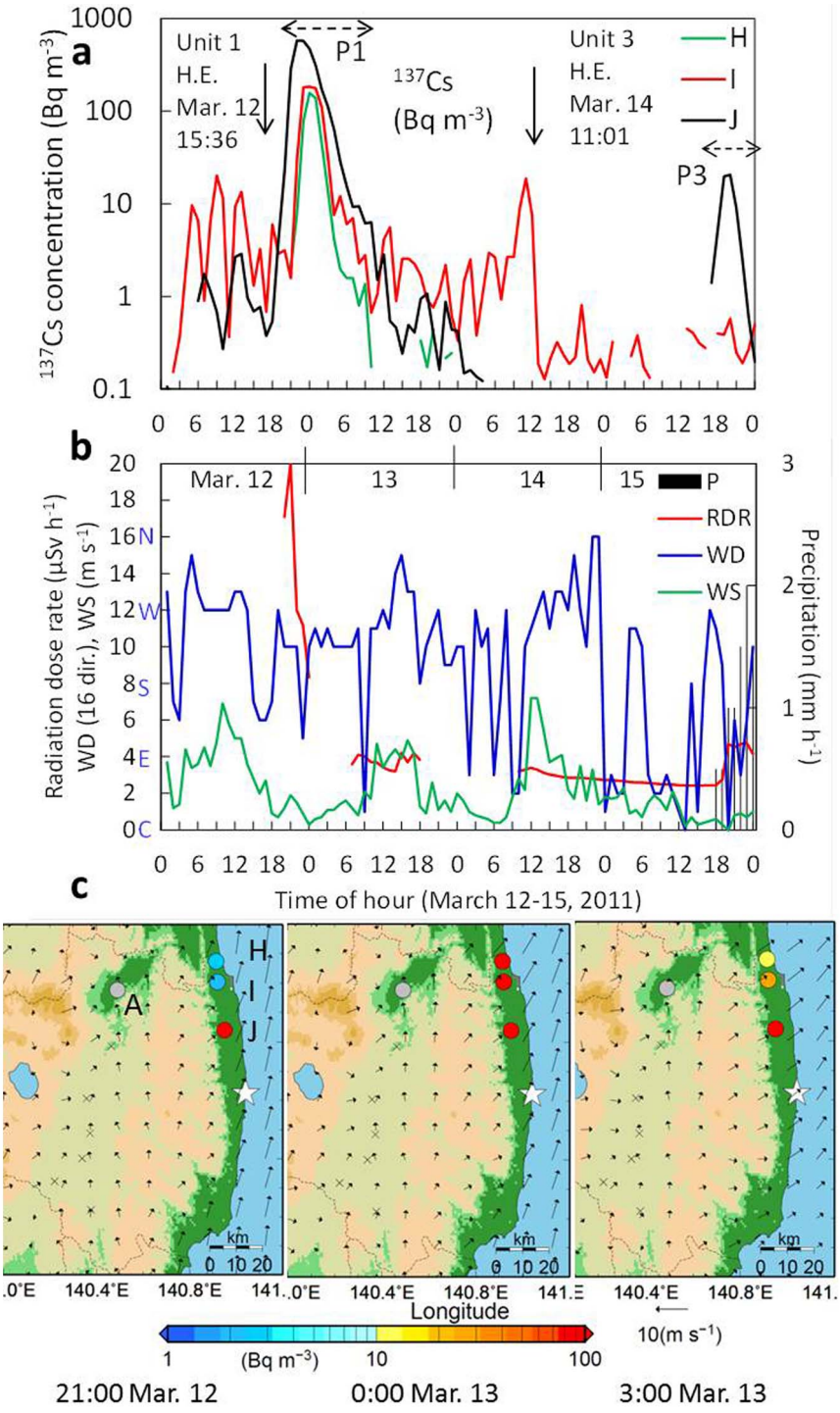

Figure 2 | P1: Spatio-temporal distribution of ^{137}Cs concentrations in northern Hamadori during March 12-15. (a), Time series of the atmospheric ^{137}Cs concentrations at sites H to J in northern Hamadori, during March 12-15. H.E., The hydrogen explosion in reactor unit 1 or 3[32]. Horizontal bars show the period with high ^{137}Cs concentrations (> 10 Bq m^{-3}). (b), Time series of radiation dose rate (RDR, red line) at the Minami-soma monitoring post near site J, precipitation (P, black and vertical line), wind direction (WD, blue line), and wind speed (WS, green line) at the Soma meteorological station near site I, during March 12–15. The right vertical axis is only for precipitation. (c), Atmospheric ^{137}Cs concentrations (colored dot) at four sites (A, H, I, and J) and wind vectors (black arrow) at 1000 hPa at 21:00 (JST), March 12, 0:00 and 3:00, March 13. The mapping of c was made by using the GMT[39] and the topography data of GTOPO30[40]. Two-dimensional wind vectors at 1000 hPa superimposed on c were made from the wind dataset of mesoscale objective analysis[38] by using wgrib2[41] and GMT[39].

polluted air masses over the Pacific Ocean (on March 14 and on March 17). The period of high ^{137}Cs concentrations was categorized into 9 plumes/polluted air masses in the chronological order (P1 to P9), as shown in Table 1. And three areas were also shown according to the transport pathways of atmospheric ^{137}Cs, (1) transport only to northern Hamadori located along the east coast of the FP in P1 (March 12–13), and P5 and P6 (March 18–19), (2) transport to Nakadori located in the central FP and northern Hamadori in P3 (March 15–16) and P8 (March 20–21), and (3) transport to the TMA in P2 (March 15), P4 (March 16), P7 (March 20), and P9 (March 21).

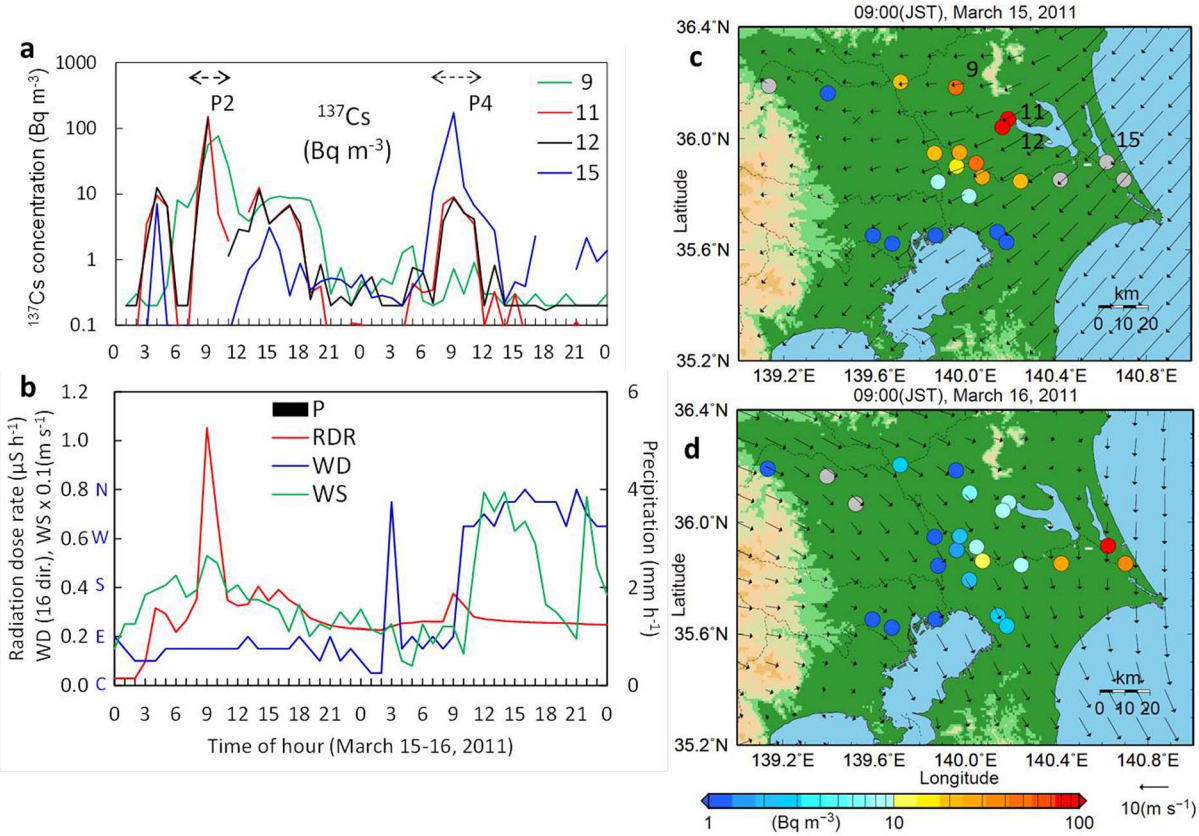

Figure 3 | P2 and P4: Spatio-temporal distribution of ^{137}Cs concentrations in TMA during March 15-16. (a), Time series of the atmospheric ^{137}Cs concentrations at 4 SPM sites (9, 11, 12, 15) in the TMA during March 15–16. Horizontal bars show the period with high ^{137}Cs concentrations (> 10 Bq m^{-3}). (b), Time series of the radiation dose rate (RDR) at Tsukuba[34], precipitation (P), wind direction (WD), and wind speed (WS) at the Tsukuba meteorological station near site 11 and 12, during March 15–16. (c), Atmospheric ^{137}Cs concentrations (colored dot) at 24 sites (1 to 24) and wind vectors (black arrow) at 1000 hPa at 9:00 (JST), March 15. (d), The same as c, but 9:00 (JST), March 16. The mapping of c and d was made by using the GMT[39] and the topography data of GTOPO30[40]. Two-dimensional wind vectors at 1000 hPa superimposed on c and d were made from the wind dataset of mesoscale objective analysis[38] by using wgrib2[41] and GMT[39].

For these periods, the spatio-temporal distributions of atmospheric ^{137}Cs were studied, with the peak ^{137}Cs concentrations and the duration of high ^{137}Cs concentrations (> 10 Bq m^{-3}) in the polluted air masses. Data analysis was not conducted for the period of March 22–23, because atmospheric ^{137}Cs concentrations did not exceed around 10 Bq m^{-3} at most of the SPM sites. In addition, the dataset from 3 sites in Aizu, the western FP (K-M, in Fig. 1b) were not analyzed in detail due to the low ^{137}Cs concentrations (< 13 Bq m^{-3}).

P1 (March 12-13): Transport to northern Hamadori. The first plume detected after the accident in this study was transported to northern Hamadori along the coast by a southerly wind, several hours after the hydrogen explosion occurred at reactor unit 1 at 15:36 (JST) on March 12[32] (Fig. 2). The ^{137}Cs concentration at site J, 25 km north of the FD1NPP, suddenly increased to more than 100 Bq m^{-3} for 7 hours after 21:00 with a maximum concentration of approximately 575 Bq m^{-3} at 22:00 and 23:00. This finding is consistent with the highest radiation dose rate of 12–20 μSv h^{-1}, which was observed at the Minami-soma monitoring post near site J[33] (Fig. 2b). At approximately 0:00 on March 13, maximum ^{137}Cs concentrations of 180 and 140–150 Bq m^{-3} were observed at the I and H sites, respectively. However, after another hydrogen explosion from reactor unit 3 at 11:01 on March 14[32], no increases in the ^{137}Cs concentration were detected at sites H-J due to a strong westerly wind.

P2 (March 15): Transport to Tokyo Metropolitan Area. On the morning of March 15 when northeasterly wind prevailed with no precipitation, the polluted air masses were transported to the TMA. And high ^{137}Cs concentrations with a maximum of 153 Bq m^{-3} were observed at site 11 (Fig. 1c) between 8:00 and 11:00 (Fig. 3a to c and Fig. S1). The polluted air masses, however, seemed to be partly transported southwestward and partly transported westward, because the wind direction in the west TMA quickly shifted clockwise.

P3 (March 15-16): Transport to Nakadori and Northern Hamadori. On March 15, radioactive materials were directly transported from the FD1NPP to Nakadori in the FP along the Abukuma highlands located at the east of Nakadori by a northeasterly wind in the morning and a southeasterly wind in the afternoon (Fig. 4). The time of the maximum ^{137}Cs concentration shifted from early afternoon in southern Nakadori (Site C to G) to the night in northern Nakadori (site A and B) (Fig. 4a and Fig. S2). At G, the southernmost site of Nakadori, the ^{137}Cs concentration increased after 9:00, and reached its maximum at 12:00 due to the transport of large amounts of radioactive materials that were released from reactor unit 2 in the early morning[32](Fig. 4a and b). Among all sites at Nakadori, a maximum ^{137}Cs concentration of 330 Bq m^{-3} was found at site E at 13:00, when no precipitation was observed. However, at site A, the northernmost part of Nakadori, the ^{137}Cs concentration began to increase from 18:00 and remained high at approximately 10 Bq m^{-3} until 3:00 in the following morning (Fig. 4c). At the same time, radiation dose rates increased up to 14–16 μSv h^{-1} due to the deposition of radioactive materials by precipitation (Fig. 4d). According to the horizontal wind

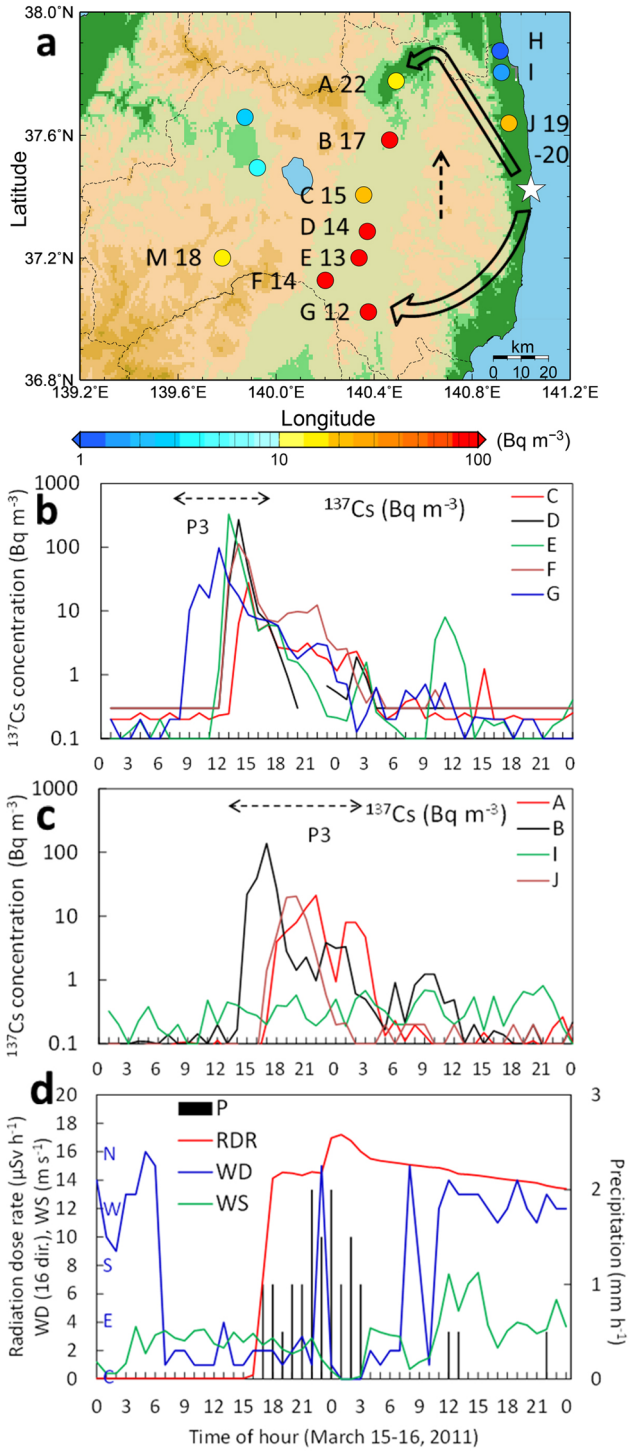

Figure 4 | P3: Time series of ^{137}Cs concentrations during March 15-16 in the FP. (a), The maximum ^{137}Cs concentration with the colored dot. The number is the time (hour) of the maximum ^{137}Cs on March 15 during the plume arrival at A to G in Nakadori and at H to J in northern Hamadori. The wide arrows show typical transport pathways of radioactive materials to southern Nakadori in the morning, and northern Nakadori in the afternoon from the FD1NPP according to the wind patterns[38]. The mapping of a was made by using the GMT[39] and the topography data of GTOPO30[40]. (b), Time series of atmospheric ^{137}Cs concentrations at sites C to G in southern Nakadori. (c), The same as b, but at sites A and B in northern Nakadori, and at I and J in northern Hamadori. (d), Time series of radiation dose rate (RDR) at the Momijiyama monitoring post located near site A, precipitation (P), wind direction (WD), and wind speed (WS) at the Fukushima meteorological station. The ^{137}Cs concentrations at sites A and C are an average ^{137}Cs concentrations at 3 and 2 sites located within 3 km each other, respectively. Horizontal bars in b and c show the periods with high ^{137}Cs concentrations (> 10 Bq m^{-3}).

distribution at 1000 hPa, the polluted air masses were transported to the Fukushima basin (Fig. S2) from the FD1NPP first by a southeasterly wind in the early afternoon. Then, the polluted air masses turned to be transported to site A in the evening by a northeasterly wind. During the night, the polluted air masses were trapped in the Fukushima basin under calm conditions until a strong northwesterly wind began to blow. However, the maximum ^{137}Cs concentration in the north was much lower than that in the south (Fig. 4b and c). In the Fukushima basin, precipitation of 1–2 mm h^{-1} was observed from 17:00 on March 15 to 03:00 on March 16 (Fig. 4d). Hence, the deposition of a large amount of ^{137}Cs on the ground by precipitation could explain the lower atmospheric ^{137}Cs concentrations in the north relative to those in the south.

P4 (March 16): Transport to eastern part of Tokyo Metropolitan Area. In the east coast area of the TMA, the ^{137}Cs concentration increased during 07:00–11:00 to show the maximum of 180 Bq m^{-3} at two SPM sites (15 and 22 in Fig. 1c) at 9:00 and 10:00 on the morning of March 16, when a northerly wind prevailed (Fig. 3d and Fig. S3). The west edge of the plume extended to the central TMA where the boundary of the two different wind directions was located. How the plume was transported from the FD1NPP is to be studied in future.

P5 and P6 (March 18-19): Transport to northern Hamadori. In northern Hamadori, the second highest ^{137}Cs concentration with the maximum of 440 Bq m^{-3} at site J (P5) was detected from 16:00 to 21:00 on March 18, when a southerly wind prevailed (Fig. 5). Furthermore, another peak of ^{137}Cs concentration of 100 to 200 Bq m^{-3} (P6) occurred at three SPM sites from 11:00 to 12:00 on March 19 (Fig. 5). The other increase (P8) which occurred on the night of March 20 will be discussed later.

P7 (March 20): Transport to Tokyo Metropolitan Area. On the afternoon of March 20, the polluted air masses with high ^{137}Cs concentrations <40 Bq m^{-3} (P7) were transported from the east coast of the TMA to the foot of mountainous area in the western TMA, when an easterly wind prevailed (Fig. 6a to c and Fig. S4). The air masses would be more aged than P2 and P4, because its width was about 40 km, equal to that of the easterly wind, and the maximum ^{137}Cs concentration was around 40 Bq m^{-3}. How the polluted air masses were transported from the FD1NPP is also to be studied in future.

P8 (March 20–21): Transport to Nakadori and northern Hamadori. In the period of March 20–21, the maximum ^{137}Cs concentration in Nakadori was firstly observed in the north on the early afternoon of March 20, due to the stronger southeasterly wind from the FD1NPP compared to that in P3 (Fig. 7a to c and Fig. S5). The high ^{137}Cs concentrations of 10–49 and 10–68 Bq m^{-3} lasted for 16 and 18 hours throughout the night at sites A and B, respectively (Fig. 7c). As well as P3, these high concentrations occurred because the polluted air masses were likely trapped under the calm conditions until a strong northwesterly wind began to blow them out in the following morning (Fig. 7d). These data revealed that the polluted air masses with high atmospheric ^{137}Cs concentrations remained in the populated area of Nakadori for more than half a day. In the south, however, the ^{137}Cs concentration only increased to 10 Bq m^{-3} due to a southeasterly wind in the early afternoon, and reached a maximum of approximately 80 Bq m^{-3} at night just after the surface wind direction shifted from the south to the north (Fig. 7a). Consequently, the maximum ^{137}Cs concentrations in Nakadori were

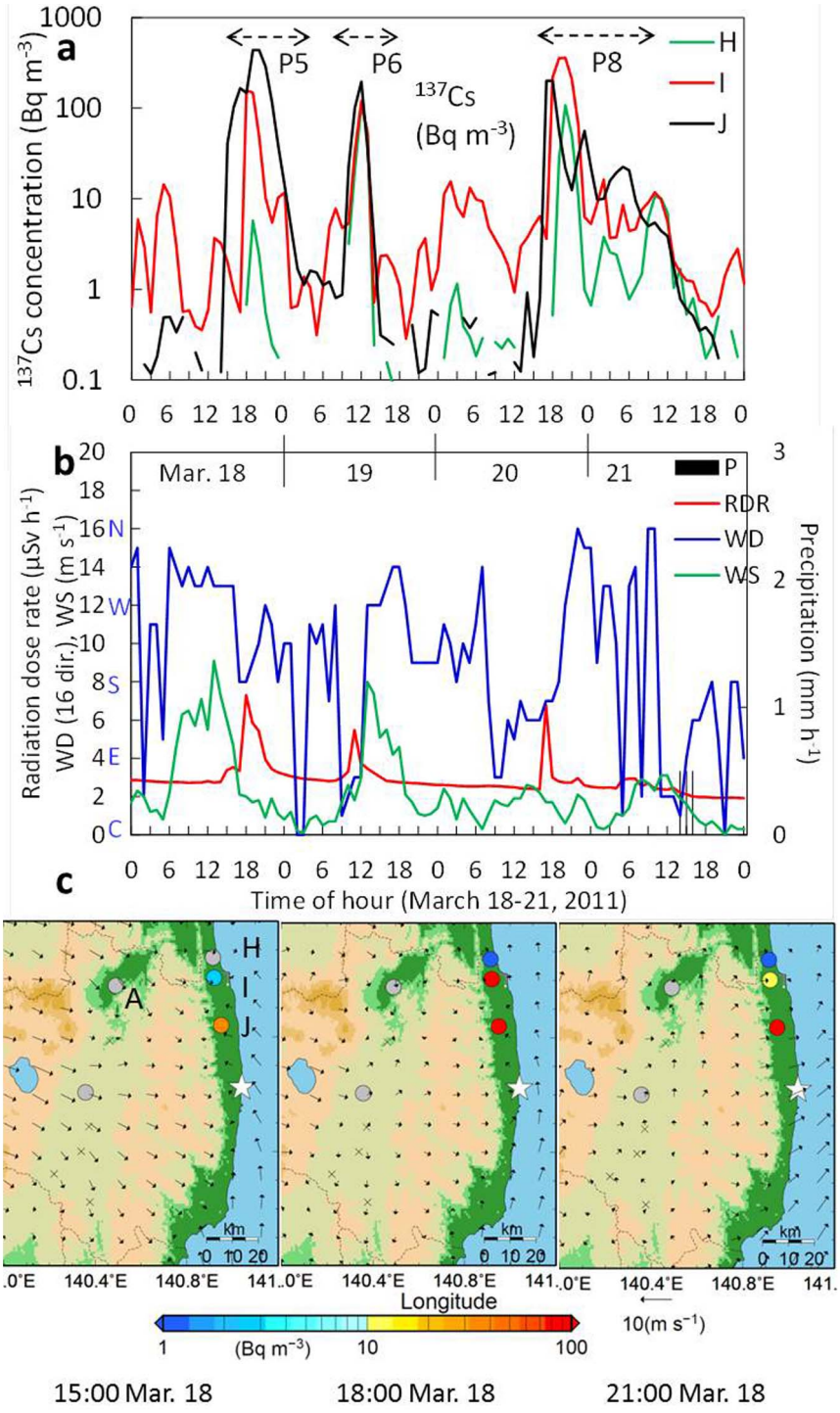

Figure 5 | P5 and P6: Spatio-temporal distribution of ^{137}Cs concentrations in northern Hamadori during March 18-21. (a) and (b), The same as Fig. 2a and b, but during March 18-21. (c), The same as Fig. 2c, but at 15:00 (JST), 18:00, and 21:00, March 18. The mapping of c was made by using the GMT[39] and the topography data of GTOPO30[40]. Two-dimensional wind vectors at 1000 hPa superimposed on c were made from the wind dataset of mesoscale objective analysis[38] by using wgrib2[41] and GMT[39].

observed later towards the south, and which was opposite compared with the P3 period (Fig. S3). The enhancement of atmospheric ^{137}Cs concentrations in Nakadori in P8, however, could not be detected by the radiation dose rates at the monitoring site, because they did not increase due to no precipitation (Fig. 7d). The dose rate had been so high by the deposit of radioactive materials on the ground by precipitation on March 15.

A much higher ^{137}Cs concentration of 60–360 Bq m^{-3} was observed between 18:00 and 22:00 on March 20 at site I in northern Hamadori, 45 km north of the FD1NPP, compared to that in Nakadori (Fig. 7c). The maximum ^{137}Cs concentration at site I was approximately 6 times higher than that measured in northern Nakadori, indicating that the fresh radionuclides released from the FD1NPP were also transported by a southerly wind as well as P1, P5 and P6.

P9 (March 21): Transport to Tokyo Metropolitan Area. After the wind direction shifted from the south to the north near the FD1NPP

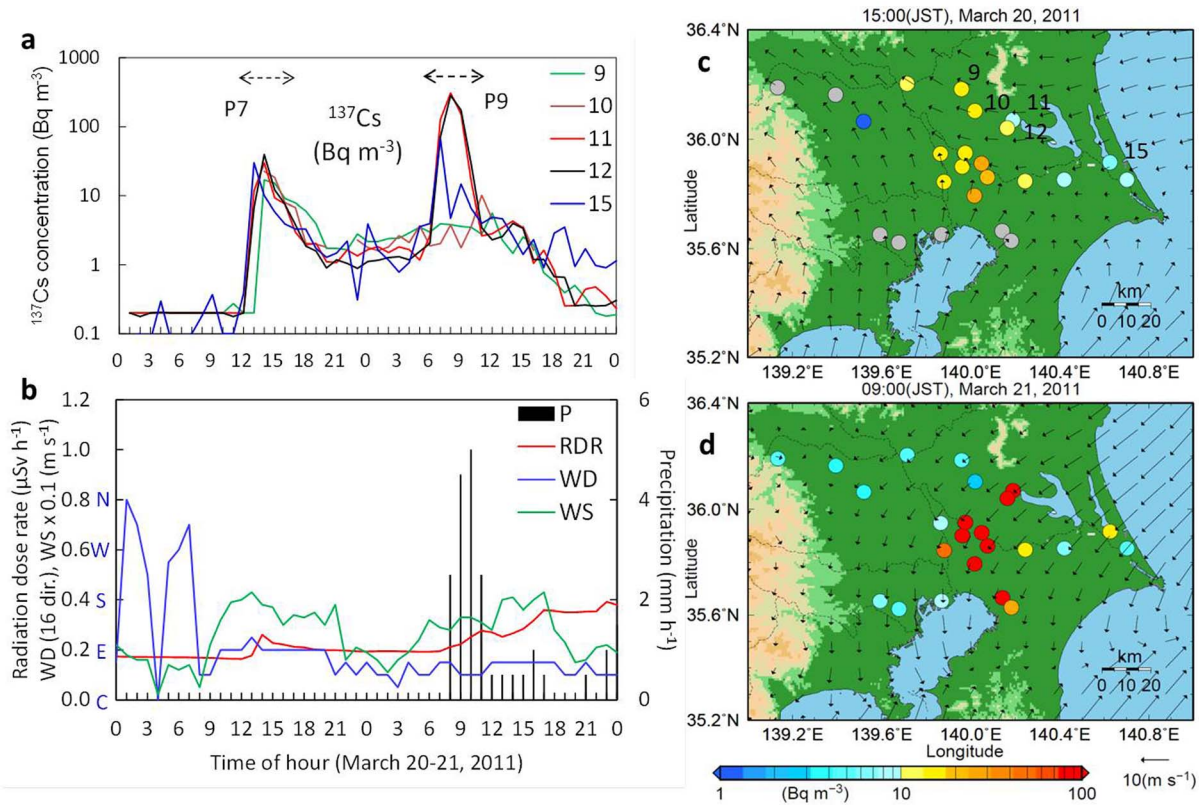

Figure 6 | P7 and P9: Spatio-temporal distribution of ^{137}Cs concentrations in TMA during March 20-21. (a), The same as Fig. 3a, but at 5 sites (9, 10, 11, 12, 15) during March 20-21. (b), The same as Fig. 3b, but during March 20-21. (c), The same as Fig. 3c, but at 15:00, March 20. (d), The same as c, but at 9:00, March 21. The mapping of c and d was made by using the GMT[39] and the topography data of GTOPO30[40]. Two-dimensional wind vectors at 1000 hPa superimposed on c and d were made from the wind dataset of mesoscale objective analysis[38] by using wgrib2[41] and GMT[39].

at 0:00 on March 21, the radioactive materials from the FD1NPP were transported southward off the east coast of the FP. A spatio-temporal distribution of the ^{137}Cs concentrations in the TMA from 7:00 to 11:00 clearly indicated that, a plume with higher ^{137}Cs concentrations ($>$ 100 Bq m^{-3}) only measured at several sites had a width of about 20 km under a constant northeasterly wind (Fig. 6d and Fig. S6). Furthermore, the spatial distribution of high ^{137}Cs changed every hour, although the ^{137}Cs concentrations before 7:00 or after 12:00 were very low at all SPM sites in the TMA. The maximum ^{137}Cs concentration was 309 Bq m^{-3} at site 11 at 8:00 when it started raining (Fig. 6a and b, and Fig. S6), comparable to that observed at site I in northern Hamadori during the previous evening (P8). The radiation dose rate at Tsukuba, however, did not increase sharply, possibly because the site was just located outside of the plume[34]. According to the vertical profile of air temperature and wind direction at Tsukuba, a strong temperature inversion layer existed at a height of 250 to 1500 m above sea level at 9:00 on March 21. It strongly suggests that the polluted air masses were transported below the inversion layer, although the thickness of the northeasterly wind in the planetary boundary layer was about 600 m.

Discussion

This study for the first time revealed the hourly transport of atmospheric ^{137}Cs from the FD1NPP to the FP and TMA just after the accident, by measuring radionuclides in the SPM collected on filter tapes installed in the SPM monitors. It also showed that site J, only 25 km north of the FD1NPP, had the highest value of the maximum and time-integrated ^{137}Cs concentration, 577 Bq m^{-3} and 5647 Bq h m^{-3}, respectively, in the early phase after the accident (March 12–23) among all the sites (Table 2). At the other sites, however, the ^{137}Cs concentrations did not depend on the distance from the FDINPP. Furthermore, the transport of the polluted air masses which was significantly different between the FP and the TMA was strongly controlled by the local/meso-scale meteorological conditions and topography. Thus, the new dataset provides the most reliable data of atmospheric ^{137}Cs concentrations for determining the initial value for internal radiation dose rates from inhalation in the early phase after the accident. To evaluate the thyroid cancer risk, the ^{131}I concentrations can be estimated spatially and temporally by using the atmospheric concentration ratio of ^{131}I to ^{137}Cs, which was observed at a few sites in the TMA[6,7].

In northern Hamadori where high ^{137}Cs concentations $>$100 Bq m^{-3} were observed in the four periods (Table 1), the ^{137}Cs deposition densities on the ground were relatively low compared to those in Nakadori where the maximum and time integrated ^{137}Cs concentrations were much lower[2–4]. The possible reason would be due to no precipitation in northern Hamadori during the four periods except for P3 with the ^{137}Cs maximum of 21 Bq m^{-3} on March 15 (Fig. 2b and Fig. 5b).

In contrast, on the morning of March 21, precipitation began at nearly the same time as the transport of the plume to the TMA, and lasted for several hours (Fig. 6b). Consequently, a large amount of radionuclides was possibly deposited on the ground by wet deposition within these several hours, compared to dry deposition on March 15 due to no precipitation. The SPM sites with high time-integrated ^{137}Cs concentrations on March 21 in the TMA were consistent with the high ^{137}Cs deposition area on the ground in the TMA, which was shown by an airborne monitoring by MEXT[35] (Fig. 8). It strongly indicates that the spatio-temporal distribution of ^{137}Cs in the atmosphere was the major factor controlling the deposition map of ^{137}Cs, because the precipitation amount on March 21 was not so

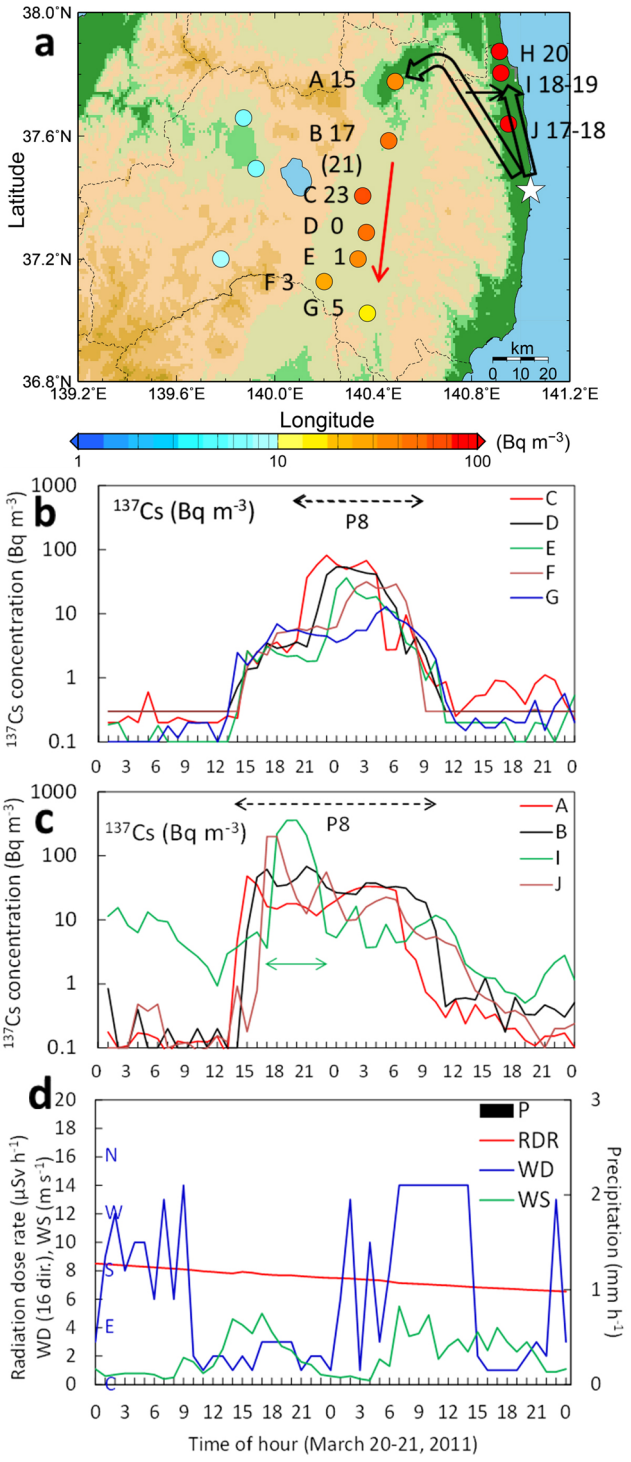

Figure 7 | P8: Time series of ^{137}Cs concentrations during March 20-21 in the FP. (a) to (d), The same as Fig. 4a to d, but during March 20-21. The wide arrows show typical transport pathways of radioactive materials to northern Nakadori in the afternoon and to northern Hamadori in the evening from the FD1NPP according to the wind patterns[38]. The red arrow in a indicates the transport pathway of the polluted air masses with the maximum ^{137}Cs concentrations when the wind direction shifted from the south to the north in the night. The mapping of a was made by using the GMT[39] and the topography data of GTOPO30[40].

different between the SPM sites located inside and outside of the plume. Thus, more appropriate parameters for dispersion and/or deposition of atmospheric ^{137}Cs in atmospheric transport and deposition models can be estimated by validating their simulated results with this new dataset. Furthermore, this hourly dataset with high time-resolution will be useful for evaluating the temporal release rate of ^{137}Cs in the source term.

Methods

SPM monitoring sites in eastern Japan. The SPM monitors in the air pollution monitoring network of Japan are routinely operated by local governments (Fig. 1a). SPM is hourly collected on filter tapes installed in the SPM monitors to measure the mass concentration of SPM by beta-ray attenuation method. A large amount of the filter tapes used at more than 400 SPM monitoring sites just after Tohoku Earthquakes and Tsunami was collected under the support from each local government in eastern Japan, and the Ministry of Environment, Japan. The SPM monitors in the FP are mainly operated in three populated areas; Nakadori is located at the center of the FP and is surrounded by the Ou Mountains on the west and by the Abukuma Highlands on the east, Hamadori is located along the east coast of the FP, and Aizu in the western FP (Fig. 1b). The Fukushima basin and site A are located in the northernmost part of Nakadori. Radionuclides in SPM were measured at all 16 sites where the used filter tapes were safely stored. In contrast, 24 SPM monitoring sites were selected for radionuclide measurements among all the SPM sites in the TMA located in the Kanto plain (Fig. 1c). The radionuclides in the hourly SPM were measured during March 12–23. In the period of March 12–14 and March 17–19, radionuclides in the SPM were detected at three sites (H–J) in northern Hamadori, because radioactive materials were only transported north or east of the FD1NPP, according to the radiation dose rates and the wind direction. In the period of March 15–16 and March 20–23, however, radionuclides were detected at many sites in the FP and TMA, because the radioactive materials released from the FD1NPP were transported to the FP and TMA, and atmospheric, aquatic, and terrestrial environments in the FP and TMA were subjected by the radioactive materials.

Measurements of radionuclides in SPM collected on filter tapes. SPM less than 10 μm in diameter was automatically collected on the filter tape as a sample spot (11 or 16 mm in diameter) for one hour at a flow rate of 15.0, 16.7 or 18.0 liters m^{-1}. The successive SPM measurements lasted for one month or more, with a single roll of filter tape made of glass fiber (GF) or polytetrafluoroethylene (PTFE). To mark the separation between two consecutive days, the same space as that of the sample spot on the filter tape is automatically fed every 24 hours without airflow. This clean space with no SPM is called a blank spot. To measure radionuclides in the SPM collected on a sample spot, the filter tape was cut at the center of a clean portion between two sample spots. After a rectangular piece including the sample spot was wrapped with a weighing paper, it was fixed on a thin plastic plate with a transparent sticker. The sample plate was subjected to gamma-spectrometry with a Ge detector. Efficiencies of the measurement for ^{134}Cs and ^{137}Cs were determined by preparing the standard samples as follows; first, standard solutions with the certified ^{134}Cs and ^{137}Cs concentrations were dropped on a paper that was the same size as the sample spot. After drying, the paper was sealed with a transparent and adhesive tape. In addition, a blank spot was measured in the same way as the sample spot. The detection limit of ^{137}Cs was approximately 0.1–0.6 Bq m^{-3} for the one-hour measurement, depending on the Ge detectors used in this study. The measurement errors corresponding to the concentration levels for ^{137}Cs were 3% for > 100 Bq m^{-3}, 3–5% for 10–100 Bq m^{-3}, 5–10% for 2–10 Bq m^{-3}, 10–20% for 0.5–2 Bq m^{-3}, and 20–60% for 0.1–0.5 Bq m^{-3}. The detailed methodology for the measurement of radiocesium has been described elsewhere[36].

We checked if the sampling system of the SPM monitors with an inlet tube of a few meters in length at a very low flow rate efficiently collected SPM including radioactive materials. The concentrations of ^{137}Cs in the SPM on a GF tape at site 6 were measured one year after sampling (Fig. 1c). At Fukazawa located 2 km southwest of site 6, Tokyo Metropolitan Industrial Technology Research Institute (TMITRI) independently collected hourly atmospheric aerosols on a GF filter just after the accident by a dust sampler without sampling tube at an airflow rate of 600 liters m^{-1}, to measure radionuclides[37]. The difference in the ^{137}Cs concentrations between these two sites was less than 10% in a range of 0.1–60 Bq m^{-3} in the period of 9:00 March 15 to 9:00 March 16 (Fig. S7). Hence, even using the sampler with a much smaller flow rate of 15 liters m^{-1} than of 600 liters m^{-1}, it was possible to achieve very precise measurements of radioactive materials in ambient air. However, the concentration of ^{137}Cs derived from filter tapes in the SPM monitors might be underestimated if ^{137}Cs-carring aerosols larger than 10 μm in diameter existed in the atmosphere.

Furthermore, we examined the maximum errors for the atmospheric ^{137}Cs concentrations due to the following cross-contamination resulted from the filter materials. Hourly sampling of the SPM with a single roll of filter tape in the SPM monitors in Japan usually lasts for one or more months. Consequently, part of the SPM collected on a sample spot may be attached on the backside of the new sample or the blank spot located one round after the previous sample spot. In general, the PTFE filters have much larger effect of the cross-contamination than the GF filters have, because (1) the thickness of the PTFE filters is about 30% of the GF filter thickness, (2) SPM can easily penetrate more deeply inside the GF filters compared with the PTFE filters due to the coarse structure, and (3) the PTFE filters have static electricity. Therefore, we selected a site using the GF filter tape, when two SPM monitoring sites, where different filter materials were used, were located near each other. For the dataset by using the PTFE filters, we carefully checked whether the ^{137}Cs concentra-

Table 2 | Range of maximum and time-integrated ^{137}Cs concentrations in the polluted air masses during March 12-21, 2011

Area (No. of dataset)	Distance from FD1NPP	Range of atmospheric ^{137}Cs concentration				
		Maximum concentrations (Range of duration, hour)				Time-integrated concentrations for 4 or 8 days
		P1 (Mar.12–13)	P2–P4 (15–16)	P5–P6 (18–19)	P7–P9 (20–21)	
	(km)	(Bq m^{-3})				(Bq h m^{-3})
N. Nakadori (2)	55–60		21–138 (5)		49–68 (16–18)	493–940
S. Nakadori (5)	60–80		28–330 (1–6)		13–81 (2–9)	357–715
N. Hamadori (3)	25–55	157–577 (5–11)	<1–21 (0–2)	108–438 (3–10)	108–360 (4–15)	911–5647
TMA (H-P9) (13)	170–210		7–175 (0–5)		68–309 (1–4)	216–970
TMA (L-P9) (11)	170–210		8–84 (0–5)		5–39 (0–5)	105–428

N., Northern; S., Southern; TMA, Tokyo Metropolitan Area; H-P9, Maximum ^{137}Cs> 50 Bq m^{-3} in P9; L-P9, Maximum ^{137}Cs< 50 Bq m^{-3} in P9; Duration, Total hours when the ^{137}Cs concentration lasted to be more than 10 Bq m^{-3}; Time-integrated concentrations for 4 or 9 days, The sum of hourly atmospheric ^{137}Cs concentrations for 4 days (Mar. 15-16 and Mar. 20-21) in N. and S. Nakadori and the TMA, or for 8 days (Mar. 12-21 except for 2 days of March 14 and March 17) in N. Hamadori; Under bar, Precipitation during the period in the area.

tion of a sample spot corresponding to the spot with the maximum ^{137}Cs concentration unreasonably increased or not due to the cross-contamination, when the plume was transported. In addition, the ^{137}Cs concentration of each blank spot was measured, because it was usually below the detection limit due to no airflow. From these measurements, the maximum cross-contamination error was estimated to be 3 and 15% of the maximum ^{137}Cs concentrations for the GF and PTFE filter tapes, respectively. The PTFE filter tape was only used at one site I among the 16 sites in the FP, and the maximum cross-contamination error was estimated to be only 5% for a ^{137}Cs concentration of 121 Bq m^{-3}, although it was estimated to be only 1.3% for the maximum concentration of 360 Bq m^{-3} when other plume passed away. In the TMA, on the other hand, the PTFE filter tape was used at 6 SPM sites, and the maximum error due to the cross-contamination was 15% for a maximum ^{137}Cs concentration of 29.4 Bq m^{-3} at site 5 (Fig. 1c). At the other sites, it was estimated to be 5.6% (71.3 Bq m^{-3} of the maximum ^{137}Cs concentration), 10% (175 Bq m^{-3}), 13% (46.9 Bq m^{-3}), 4.0% (138 Bq m^{-3}), and 7.2% (148 Bq m^{-3}), at site 7, 15, 16, 21, and 22, respectively. Thus, the maximum error for the PTFE filter tapes due to the cross-contamination was at random, and not systematic. It could depend on environmental conditions, such as the winding strength of the PTFE filter tape. In conclusion, the cross-contamination error was too difficult to be corrected properly. Hence, the true value of a maximum ^{137}Cs concentration at each SPM site with the PTFE filter, could be higher than the measured value, depending on the each cross-contamination error.

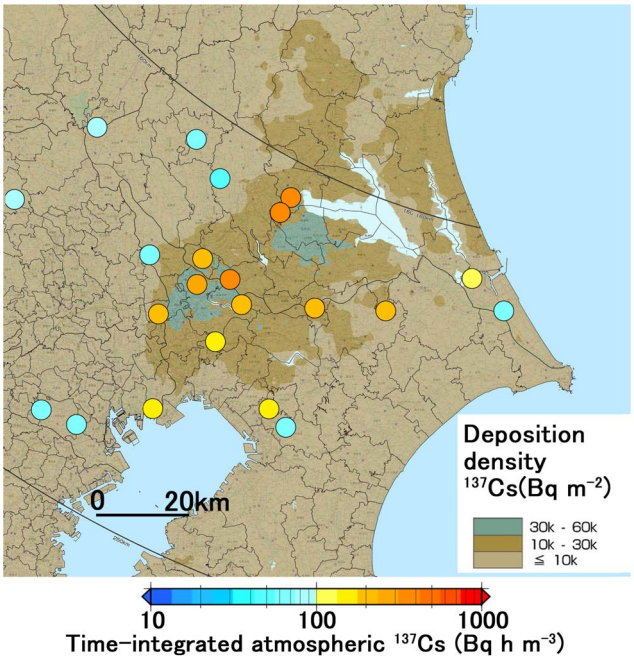

Figure 8 | Time-integrated atmospheric concentrations and deposition map for ^{137}Cs in the TMA. A spatio-distribution of time-integrated atmospheric ^{137}Cs concentrations (colored dot) on March 21 at 22 sites in the TMA, is superimposed on the ^{137}Cs deposition map, which is composed of 12 extension site maps (Site No. is 5339-C, 5339-D, 5340-A, 5340-B, 5340-C, 5340-D, 5439-C, 5439-D, 5440-A, 5440-B, 5440-C, and 5440-D) in airborne monitoring by MEXT[35]. The deposition density of ^{137}Cs converted as of September 18, 2011 was used. The colored circles were made by using the GMT[39]. The mapping of the figure, combining 12 site maps into one figure, and on which the colored circles were put, was made by using the Adobe Photoshop CS6.

Meteorological and radiation dose rate data. A map of wind distribution at a height of 1000 hPa every three hours in March 2011 was used, which was calculated with mesoscale objective analysis by the Japan Meteorological Agency (JMA)[38]. In addition, the surface and upper meteorological data were used at the Fukushima, Soma and Tsukuba stations in the Automated Meteorological Data Acquisition System (AMeDAS) network by the JMA (Fig. 1b and c). Furthermore, a map of precipitation was used which was analyzed every 30 minutes by radar and AMeDAS data by the JMA. Hourly radiation dose rates were used, at Momijiyama Park in Fukushima city, and at Minami-soma in northern Hamadori 25 km north of the FD1NPP, in the monitoring post network by the FP[33], and at the High Energy Accelerator Research Organization (KEK) in Tsukuba, located 15 km north of the Tsukuba AMeDAS station[34].

1. Ministry of Education, Culture, Sports, Science and Technology. Readings of environmental radioactivity level by prefecture (March 2011). http://radioactivity.nsr.go.jp/ja/list/224/list-201103.html (The last date of access: 25 March 2014).
2. Ministry of Education, Culture, Sports, Science and Technology. Preparation of Distribution Map of Radiation Doses, etc. (Map of Radioactive Cesium Concentration in Soil) by MEXT (2011). http://radioactivity.nsr.go.jp/en/contents/5000/4165/24/1750_083014.pdf (Date of access: 12 March 2014).
3. Ministry of Education, Culture, Sports, Science and Technology. Results of the fourth airborne monitoring survey by MEXT (2011). http://radioactivity.nsr.go.jp/en/contents/4000/3179/24/1270_1216.pdf (Date of access: 4 March 2014).
4. Torii, T., Sugita, T., Okada, C., Reed, M. & Blumenthal, D. Enhanced analysis methods to derive the spatial distribution of ^{131}I deposition on the ground by airborne surveys at an early stage after the Fukushima Daiichi Nuclear Power Plant accident. *Health Phys.* **105**, 192–200 (2013).
5. Saito, K. *et al.* Detailed deposition density maps constructed by large-scale soil sampling for gamma-ray emitting radioactive nuclides from the Fukushima Daiichi Nuclear Power Plant accident. *J. Environ. Radioact.* DOI: 10.1016/j.jenvrad.2014.02.014 (2014). (in press).
6. Furuta, S. *et al.* Results of the environmental radiation monitoring following the accident at the Fukushima Daiichi Nuclear Power Plant. JAEA-Review 2011-035 (2011). (in Japanese with English abstract). http://jolissrch-inter.tokai-sc.jaea.go.jp/pdfdata/JAEA-Review-2011-035.pdf (Date of access: 5 July 2012).
7. Tsuruta, H., Takigawa, M. & Nakajima, T. Summary of atmospheric measurements and transport pathways of radioactive materials released by the Fukushima Daiichi Nuclear Power Plant accident. [Proceedings on the 1st NIRS Symposium on Reconstruction of Early Internal Dose in the TEPCO Fukushima Daiichi Nuclear Power Station Accident.] [Kurihara, O. *et al* (eds.)] [101–111] (National Institute of Radiological Sciences, Chiba, 2012).
8. Chino, M. *et al.* Preliminary estimation of release amounts of ^{131}I and ^{137}Cs accidentally discharged from the Fukushima Daiichi nuclear power plant into the atmosphere. *J. Nucl. Sci. Technol.* **48**, 1129–1134 (2011).
9. Stohl, A. *et al.* Xenon-133 and caesium-137 releases into the atmosphere from the Fukushima Dai-ichi nuclear power plant: determination of the source term, atmospheric dispersion, and deposition. *Atmos. Chem. Phys.* **11**, 28319–28394 (2011).
10. Katata, G., Terada, H., Nagai, H. & Chino, M. Numerical reconstruction of high dose rate zones due to the Fukushima Dai-ichi Nuclear Power Plant accident. *J. Environ. Radioact.* **111**, 2–12 (2012).

11. Katata, G., Ota, M., Terada, H., Chino, M. & Nagai, H. Atmospheric discharge and dispersion of radionuclides during the Fukushima Dai-ichi Nuclear Power Plant accident: Part I: Source term estimation and local scale atmospheric dispersion in early phase of the accident. *J. Environ. Radioact.* **109**, 103–113 (2012).
12. Winiarek, V., Boquet, M., Saunier, O. & Mathieu, A. Estimation of errors in the inverse modeling of accidental release of atmospheric pollutant: Application to the reconstruction of cesium-137 and iodine-131 source terms from the Fukushima Daiichi power plant. *J. Geophys. Res.* **117**, D05122; DOI:10.1029/2011JD016932 (2012).
13. Terada, H., Katata, G., Chino, M. & Nagai, H. Atmospheric discharge and dispersion of radionuclides during the Fukushima Daiichi Nuclear Power Plant accident. Part II: Verification of the source term and regional-scale atmospheric dispersion. *J. Environ. Radioact.* **112**, 141–154 (2012).
14. Kobayashi, T., Nagai, H., Chino, M. & Kawamura, H. Source term estimation of atmospheric release due to the Fukushima Dai-ichi Nuclear Power Plant accident by atmospheric and oceanic dispersion simulations. *J. Nucl. Sci. Technol.* **50**, 255–264; DOI:10.1080/00223131.2013.772449 (2013).
15. Takemura, T. *et al.* A numerical simulation of global transport of atmospheric particles emitted from the Fukushima Daiichi Nuclear Power Plant. *SOLA.* **7**, 101–104; DOI:10.2151/sola.2011-026 (2011).
16. Morino, Y., Ohara, T. & Nishizawa, M. Atmospheric behavior, deposition and budget of radioactive materials from Fukushima Daiichi nuclear power plant in March 2011. *Geophys. Res. Lett.* **38**, L00G11; DOI: 10.1029/2011GL048689 (2011).
17. Mathieu, A. *et al.* Atmospheric dispersion and deposition of radionuclides from the Fukushima Daiichi nuclear power plant accident. *Elements* **8**, 195–200; DOI: 10.2113/gselements.8.3.195 (2012).
18. Draxler, R. R. & Rolph, G. D. Evaluation of the Transfer Coefficient Matrix (TCM) approach to model the atmospheric radionuclide air concentrations from Fukushima. *J. Geophys. Res.* **117**, D05107; DOI:10.1029/2011JD017205 (2012).
19. Sugiyama, G. *et al.* Atmospheric dispersion modeling: Challenges of the Fukushima Daiichi response. *Health Phys.* **102**, 493–508 (2012).
20. Srinivas, C. V., Venkatesan, R., Baskaran, R., Rajagopal, V. & Venkatraman, B. Regional scale atmospheric dispersion simulation of accidental releases of radionuclides from Fukushima Dai-ichi reactor. *Atmos. Environ.* **61**, 66–84 (2012).
21. Nagai, H., Chino, M., Terada, H. & Katata, G. Atmospheric dispersion simulations of radioactive materials discharged from the Fukushima Daiichi Nuclear Power Plant due to the accident: Consideration of deposition process. [Proceedings on the 1st NIRS Symposium on Reconstruction of Early Internal Dose in the TEPCO Fukushima Daiichi Nuclear Power Station Accident.] [Kurihara, O. *et al* (eds)] [137–149] (National Institute of Radiological Sciences, Chiba, 2012).
22. Morino, Y., Ohara, T., Watanabe, M., Hayashi, S. & Nishizawa, M. Episode analysis of deposition of radiocesium from the Fukushima Daiichi Nuclear Power Plant Accident. *Environ. Sci. Technol.* **47**, 2314–2322 (2013).
23. Draxler, R. *et al.* World Meteorological Organization's model simulations of the radionuclide dispersion and deposition from the Fukushima Daiichi nuclear power plant accident. *J. Environ. Radioact.* (in press) http://dx.doi.org/10.1016/j.jenvrad.2013.09.014 (2013). (Date of access: 26 March 2014).
24. Christoudias, T. & Lelieveld, J. Modelling the global atmospheric transport and deposition of radionuclides from the Fukushima Dai-ichi nuclear accident. *Atmos. Chem. Phys.* **13**, 1425–1438; DOI:10.5194/acp-13-1425-2013 (2013).
25. World Health Organization. *Preliminary dose estimation from the nuclear accident after 2011 Great East Japan Earthquake and Tsunami* (WHO Press, Geneva, 2012).
26. Tokonami, S. *et al.* Thyroid doses for evacuees from the Fukushima nuclear accident. *Sci. Rep.* **2**, 507; DOI:10.1038/srep00507 (2012).
27. Kim, E. *et al.* Screening survey on thyroid exposure for children after the Fukushima Daiichi nuclear power plant station accident. [Proceedings on the 1st NIRS Symposium on Reconstruction of Early Internal Dose in the TEPCO Fukushima Daiichi Nuclear Power Station Accident.] [Kurihara, O. *et al* (eds)] [59–66] (National Institute of Radiological Sciences, Chiba, 2012).
28. World Health Organization. *Health risk assessment from the nuclear accident after 2011 Great East Japan Earthquake and Tsunami based on a preliminary dose estimation* (WHO Press, Geneva, 2013).
29. Matsuda, N. *et al.* Assessment of internal exposure doses in Fukushima by a whole body counter within one month after the nuclear power plant accident. *Rad. Res.* **179**, 663–668 (2013).
30. Morita, N. *et al.* Spatiotemporal characteristics of internal radiation exposure in evacuees and first responders after the radiological accident in Fukushima. *Rad. Res.* **180**, 299–306 (2013).
31. Cooper, J. R., Randle, K. & Sokhi, R. S. *Radioactive Releases in the Environment: Impact and Assessment.* [407] (John Wiley & Sons, England, 2003).
32. Tokyo Electric Power Company. Fukushima Nuclear Accidents Investigation Report (2012). http://www.tepco.co.jp/en/press/corp-com/release/2012/1205638_1870.html. (Date of access: 21 June 2012).
33. Fukushima prefecture. Radiation dose rates at the monitoring posts in Fukushima prefecture (2013). http://www.atom-moc.pref.fukushima.jp/monitoring/monitoring201103/201103_mpdata.html. (The last date of access: 6 December 2013).
34. Sanami, T., Sasaki, S., Iijima, K., Kishimoto, Y. & Saito, K. Time variations in dose rate and γ spectrum measured at Tsukuba city, Ibaraki, due to the accident of Fukushima Daiichi Nuclear Power Station. *Transactions of the Atomic Energy Society of Japan,* **10**, 163–169 (2011). (in Japanese with English abstract).
35. Ministry of Education, Culture, Sports, Science and Technology. Extension Site of Distribution Map of Radiation Dose etc.,/Digital Japan (2011). http://ramap.jmc.or.jp/map/eng/. (Date of access: 4 January 2013).
36. Oura, Y. *et al.* Determination of atmospheric radiocesium on filter tapes used at automated SPM monitoring stations for estimation of transport pathways of radionuclides from Fukushima Dai-ichi Nuclear Power Plant. *J. Radioanal. Nucl. Chem.* (accepted).
37. Tokyo Metropolitan Government. Measurement of nuclear fission products of dust particles in the air in Tokyo (2011). http://www.sangyo-rodo.metro.tokyo.jp/whats-new/keisoku-0323-0315.pdf. (Date of access:28 March 2012).
38. Japan Meteorological Agency. *Mesoscale objective analysis, March 2011.* (Japan Meteorological Business Support Center, Tokyo, 2012).
39. Wessel, P. & Smith, W. H. F. New, improved version of the Generic Mapping Tools released. *EOS Trans. AGU,* **79**, 579 (1998). http://onlinelibrary.wiley.com/doi/10.1029/98EO00426/abstract. (The last date of access: 19 April 2014).
40. U.S. Geological Survey. Global 30 Arc-Second Elevation (GTOPO30) (1996). https://lta.cr.usgs.gov/GTOPO30. (The last date of access: 19 May 2013).
41. National Oceanic and Atmospheric Administration. wgrib2: -rpn. Climate Prediction Center (2013). http://www.cpc.noaa.gov/products/wesley/wgrib2/rpn.html. (Date of access: 8 October 2013).

Acknowledgments

We thank to the local government of Fukushima, Ibaraki, Saitama, Chiba, and Tokyo, and the city of Koriyama, Iwaki, Chiba, and Kashiwa for allowing us to measure radionuclides in the SPM collected on the used filter tapes in the SPM monitors. We also thank S.Wakamatsu (Ehime University), and many other persons who cooperated to store the filter tapes. We sincerely acknowledge Y. Katsumura and M. Ishimoto in The University of Tokyo for supporting the measurements. We also acknowledge K. Shiba and Y. Kusama in The University of Tokyo for mapping in the figures. This work was partly supported by the "Interdisciplinary Study on Environmental Transfer of Radionuclides from the Fukushima Daiichi NPP Accident" project by JSPS KAKENHI (Grant Numbers are 24110002, 24110008, and 24110009), and by the "Development of Seamless Chemical Assimilation System and its Application for Atmospheric Environmental Materials (SALSA)" project in the Research Program on Climate Change Adaptation (RECCA) by MEXT, and by the "Active evaluation of the environmental effects caused by greenhouse gases and short-lived climate pollutants" project (S-12) in ERTDF by the Ministry of Environment, Japan. It was also partly supported by the "Measurements and Distribution Map of Radionuclides by using the Filter Tapes in SPM Monitors" project by the Ministry of Environment, Japan (2012).

Author contributions

H.T. initiated and designed the research program. Y.O. was responsible for the radionuclide measurements by the Ge detectors, and was supported by H.T. and M.E. H.T. analyzed the data and wrote the manuscript with contributions from T.N., M.E., T.O. and Y.O.

Additional information

Supplementary information accompanies this paper at http://www.nature.com/scientificreports

Competing financial interests: The authors declare no competing financial interests.

How to cite this article: Tsuruta, H., Oura, Y., Ebihara, M., Ohara, T. & Nakajima, T. First retrieval of hourly atmospheric radionuclides just after the Fukushima accident by analyzing filter-tapes of operational air pollution monitoring stations. *Sci. Rep.* **4**, 6717; DOI:10.1038/srep06717 (2014).